Optical and magnetic spectroscopy of rare-earth-doped yttrium aluminium borate ($YAl_3(BO_3)_4$) single crystals

2003 J. Phys.: Condens. Matter 15 3323

(http://iopscience.iop.org/0953-8984/15/19/331)

INSTITUTE OF PHYSICS PUBLISHING JOURNAL OF PHYSICS: CONDENSED MATTER

J. Phys.: Condens. Matter **15** (2003) 3323–3331 PII: S0953-8984(03)59754-5

Optical and magnetic spectroscopy of rare-earth-doped yttrium aluminium borate ($YAl_3(BO_3)_4$) single crystals

A Watterich[1], P Aleshkevych[2], M T Borowiec[2], T Zayarnyuk[2], H Szymczak[2], E Beregi[1] and L Kovács[1]

[1] Research Institute for Solid State Physics and Optics, Konkoly-Thege M. út 29-33, 1121 Budapest, Hungary
[2] Institute of Physics, Polish Academy of Sciences, Aleja Lotników 32/46, 02-668 Warsaw, Poland

E-mail: watter@szfki.hu

Received 19 February 2003
Published 6 May 2003
Online at stacks.iop.org/JPhysCM/15/3323

Abstract
For Ce^{3+}, Er^{3+} and Yb^{3+} ions, electron paramagnetic resonance (EPR) spectra typical for $S' = 1/2$ ions are measured for $YAl_3(BO_3)_4$ (YAB) single crystal. The spectra show axial symmetry indicating that all three dopants replace Y^{3+} at the given dopant concentration. Corresponding $\tilde{\mathbf{g}}$- and hyperfine $\tilde{\mathbf{A}}$-tensors are determined. The EPR linewidth of Ce broadens with increasing temperature due to an Orbach relaxation process. Fitting the curve with an exponential, the energy difference is found to be equal to 270 ± 16 cm^{-1}.

The optical absorption and excitation spectra of Ce in YAB single crystal measured at 300 K are similar to those found for polycrystalline materials. High-resolution polarized emission from the lowest excited to the $^2F_{5/2}$ ground state, measured at 4.2 K, indicates a splitting of the ground state into three levels. The second level is located 277 ± 18 cm^{-1} above the first one, in excellent agreement with the EPR result, and the third level is located 140 ± 10 cm^{-1} above the second one.

1. Introduction

Yttrium aluminium borate ($YAl_3(BO_3)_4$, often abbreviated as YAB) is a non-linear optical material with excellent chemical and physical properties, such as wide optical transparency, even towards the UV range. It is a possible self-frequency-doubling UV–visible laser material when doped with rare-earth ions [1]. The optical spectra of Nd^{3+} (absorption and photoluminescence [2]), Er^{3+} (absorption [3]) and Yb^{3+} (absorption and photoluminescence [4]) in single crystals and Ce^{3+} in polycrystalline powder samples [5, 6] were studied. In [5] only three, while in [6] five different excitation bands were reported.

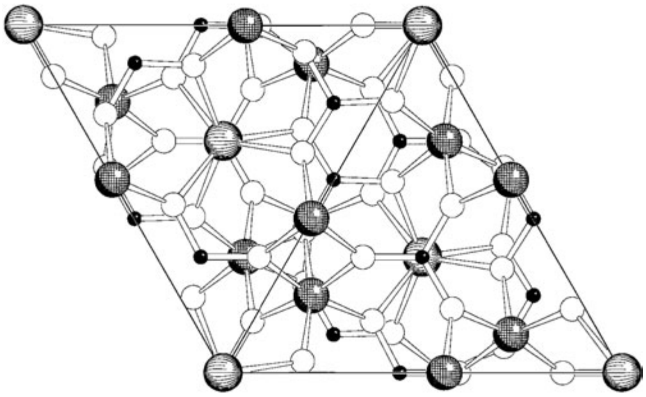

Figure 1. The model of YAB crystal lattice projected onto the (0001) plane. Striped, cross-hatched, full and open circles represent Y, Al, B and O ions, respectively.

Ce in YAB was concluded to be a good candidate for use as a detector of scintillation of thermal neutrons or alpha particles because of its large boron weight fraction (12%) which is the highest among the orthoborates [7]. Surprisingly, no EPR studies were found related to rare-earth elements in YAB.

The aim of this work is to characterize the Ce^{3+}, Er^{3+} and Yb^{3+} ions in YAB single crystal with EPR spectroscopy. Since the linewidth of the Ce^{3+} EPR showed temperature broadening indicating an Orbach relaxation process, our Ce studies were completed with optical investigations.

2. Experimental and crystal structure

0.01 rare-earth atom per YAB molecule was added to the starting material and the crystal samples were grown by spontaneous nucleation from $K_2Mo_3O_{10}$–B_2O_3 flux or from the same flux by the high-temperature top-seeded solution method. The EPR measurements were carried out with an X-band spectrometer. To fit the experimental data, the computer program 'VisualEPR' devised by Grachev was used. For optical absorption and photoluminescence measurements at $\sim$300 K, Jasco UV–VIS 550 and Hitachi F-4500 spectrometers, respectively, were used. Polarized emission measurements were made using a home-built optical system (with monochromator SPM2, exciting Xe lamp A-1010B from Photon Technology International, Canada, photomultiplier EMI with a photocathode of S20 type and lock-in amplifier EG&G PAR model 5209). Low-temperature spectra were measured with an Oxford Instruments continuous-flow cryostat Model 1104 working in the range 3.5–500 K.

YAB belongs to the group of double borates having trigonal structure characterized by the space group $R32$; its crystallographic parameters are given in [8]. There are two different boron sites (with C_3 and C_2 point symmetry, respectively), three differently oriented but energetically equivalent Al sites (C_2 symmetry) and only one Y site with D_{3h} symmetry. Figure 1 shows the crystal model projected onto the (0001) plane.

3. Results and discussion

3.1. Electron paramagnetic resonance (EPR)

Ce^{3+}, Er^{3+} and Yb^{3+} ions in YAB have a single EPR spectrum typical for $S' = 1/2$ ions occupying a single lattice site. Neglecting the hyperfine (HF) structure, these spectra consist

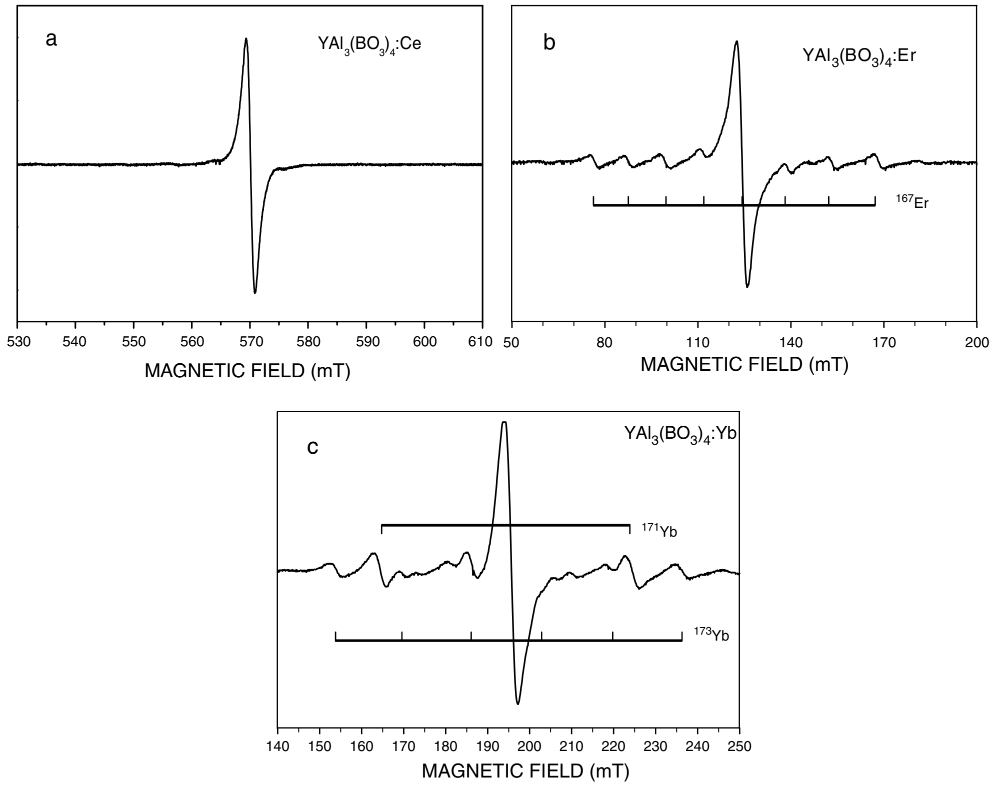

Figure 2. EPR spectra of Ce^{3+} (a), Er^{3+} (b) and Yb^{3+} (c) ions in YAB single crystals measured at 16, 16 and 9 K, respectively, and 9.24 GHz.

of one line (figures 2(a)–(c)). Ce isotopes with non-zero natural abundances have no nuclear spins and therefore no HF interaction is expected (figure 2(a)). However, some of the Er and Yb isotopes have nuclear spins: ^{167}Er with $I = 7/2$ (natural abundance 22.9%); ^{171}Yb with $I = 1/2$ (14.4%); and ^{173}Yb with $I = 5/2$ (16.2%). Figures 2(b) and (c) show the EPR spectra of Er and Yb ions in YAB, respectively. The central lines arise from those isotopes that have no nuclear spin. For the ^{167}Er isotope with $I = 7/2$, ^{171}Yb with $I = 1/2$ and ^{173}Yb with $I = 5/2$, eight, two and six HF lines are observed for the allowed transitions $\Delta m_s = \pm 1$ and $\Delta m_I = 0$, respectively. The HF lines are marked in the figures. The intensity ratios of HF (I) and central (I_c) lines can be calculated by using the natural abundances as probabilities (P); for example, for Er: $I/I_c = P_I/nP_{I_c} = 0.229/8 \times 0.771 = 1/27$, where $n = 2I + 1$ is the number of HF transitions. The ratio of the line intensities of the two Yb isotopes is $I_{1/2}/I_{5/2} = 0.144/2 \times 6/0.162 = 2.67$ which is approximately observed.

For all observed dopants, both **g**- and HF $\tilde{\mathbf{A}}$-tensors are isotropic in the (0001) plane, while strong anisotropy is observed when rotating the magnetic field $\boldsymbol{B}$ from the [0001] crystallographic direction towards the (0001) plane. Figures 3(a), (b) and 4(a), (b) show the angular variations of the Ce^{3+} and Er^{3+} line positions in two different planes, respectively. The spin-Hamiltonian parameters have been determined using the following spin Hamiltonian:

$$\boldsymbol{H}_S = \mu_B \boldsymbol{S}' \cdot \tilde{\mathbf{g}} \cdot \boldsymbol{B} + \boldsymbol{S}' \cdot \tilde{\mathbf{A}} \cdot \boldsymbol{I} - g_N \mu_N \boldsymbol{B} \cdot \boldsymbol{I}. \tag{1}$$

Here $\tilde{\mathbf{g}}$ and $\tilde{\mathbf{A}}$ are the g-tensor and the HF tensor, $\boldsymbol{S}'$ is the effective spin which is equal $1/2$ for all dopants investigated ($4f^1$, $4f^{11}$ and $4f^{13}$ electron configurations for Ce^{3+}, Er^{3+} and Yb^{3+},

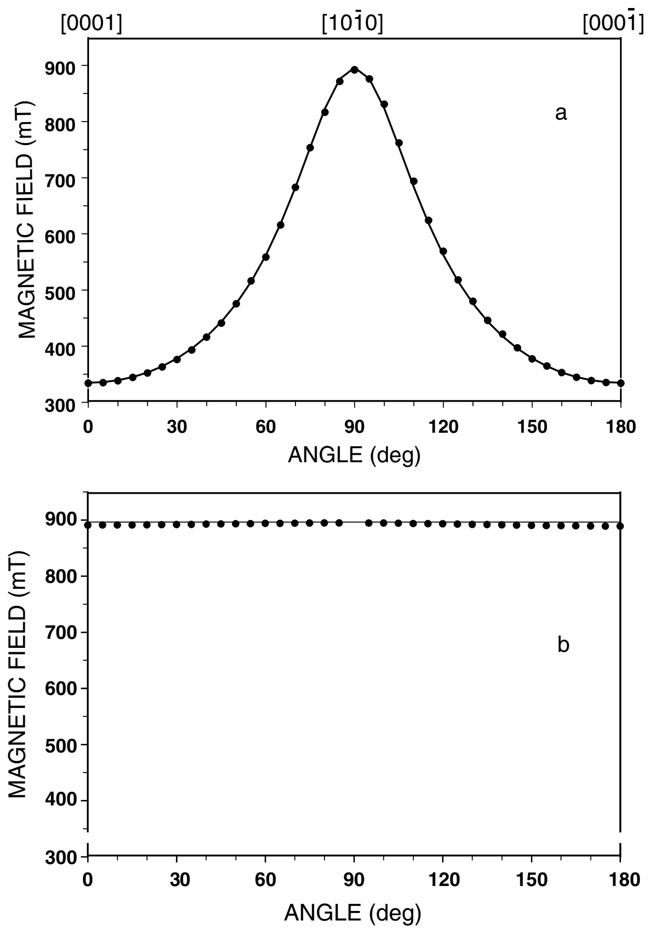

Figure 3. Angular variations of the EPR line of Ce in YAB single crystal, where symbols and solid curves represent experimental data and line positions calculated from the optimized spin-Hamiltonian parameters, respectively. The angles 0°, 90° and 180° correspond in (a) to $\boldsymbol{B}$ along [0001], [10$\bar{1}$0] and [000$\bar{1}$], respectively, while in (b), where $\boldsymbol{B}$ is rotated in the (0001) plane, 0° corresponds to [10$\bar{1}$0].

Table 1. Spin-Hamiltonian parameters for rare-earth ions in YAB.

Ion	$g_{\parallel}$	$g_{\perp}$	$A_{\parallel}$	$A_{\perp}$
Ce^{3+} ($4f^1$)	1.972 ± 0.001	0.737 ± 0.001	—	—
Er^{3+} ($4f^{11}$)	1.348 ± 0.003	9.505 ± 0.02	58.5 ± 2.8	333.3 ± 0.6
Yb^{3+} ($4f^{13}$)	3.612 ± 0.001	1.702 ± 0.001	958 ± 1.6	454 ± 3.4

respectively), $\boldsymbol{I}$ is the particular nuclear spin. For Yb only the HF lines of the ^{171}Yb isotope have been studied in detail. In figures 3, 4, symbols represent experimental data and the solid curves are calculated using the optimized spin-Hamiltonian parameters. Table 1 shows the fitted spin-Hamiltonian parameters. The observed symmetry of the EPR spectra is axial for all observed dopants.

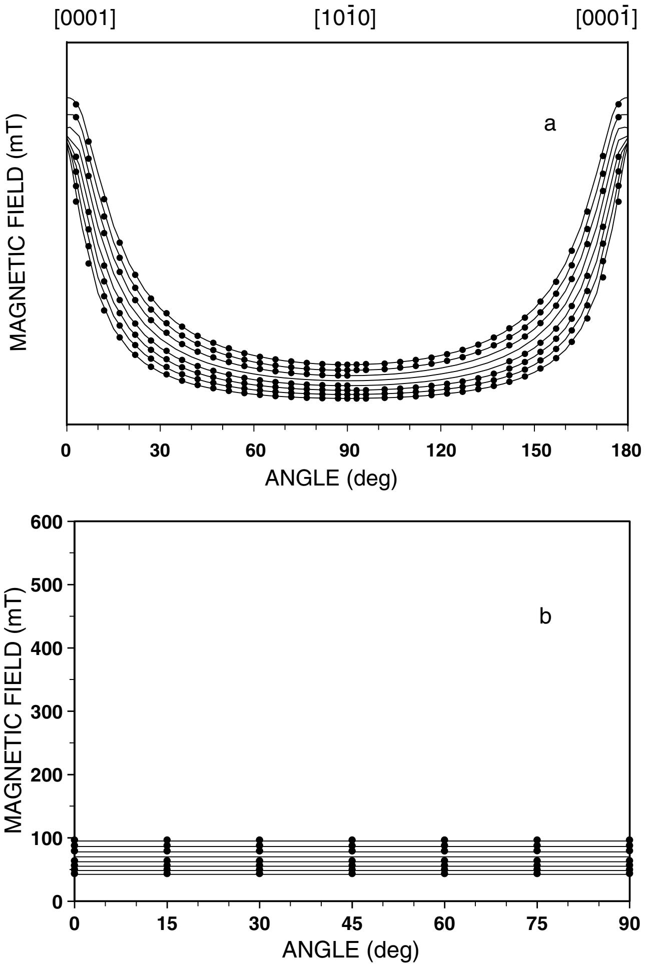

Figure 4. Angular variations of the HF lines of the ^{167}Er isotope ($I = 7/2$) in YAB single crystal, where symbols and solid curves represent experimental data and line positions from the optimized spin-Hamiltonian parameters, respectively. The angles 0°, 90° and 180° correspond in (a) to $\boldsymbol{B}$ along [0001], [10$\bar{1}$0] and [000$\bar{1}$], respectively, while in (b), where $\boldsymbol{B}$ is rotated in the (0001) plane, 0° corresponds to [10$\bar{1}$0].

Y is the only host cation in YAB having a single site and its site symmetry is D_{3h} which should manifest itself in axial symmetry of the EPR spectra. The observed symmetry indicates that the rare-earth ions studied at the given concentration replace Y. No other lines indicating different substitution were observed. The Y replacement is reasonable comparing the ionic radii of Ce^{3+}, Er^{3+} and Yb^{3+} (0.102, 0.096 and 0.094 nm, respectively) with those of the host cations Y^{3+}, Al^{3+} and B^{3+} (0.093, 0.051 and 0.022 nm, respectively). The relatively large rare-earth ions will substitute for the large Y^{3+} rather than for the much smaller Al^{3+} or B^{3+} ions.

Photoluminescence studies showed that Eu^{3+} had D_3 symmetry instead of D_{3h} due to a slight change of the orientation of borate groups around the Eu ion substituting for Y [9]. Both symmetries lead to axial symmetry in EPR; therefore this method cannot distinguish between them.

The EPR linewidths of rare-earth ions are fairly temperature dependent. Figure 5 shows the change of the linewidth (ΔH) versus reciprocal temperature for Ce in YAB. The dependence

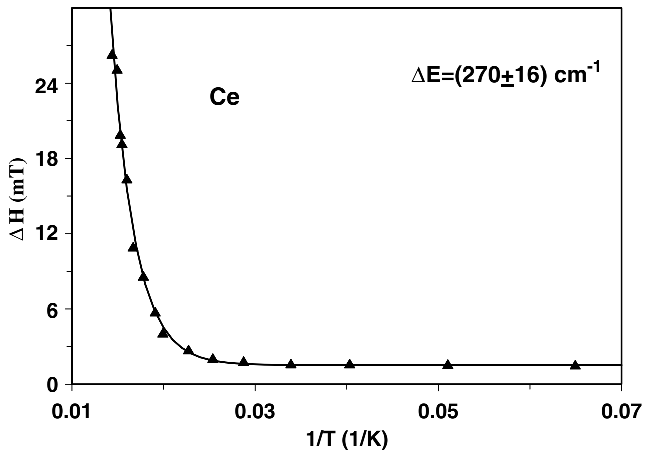

Figure 5. The temperature dependence of the EPR linewidth of Ce^{3+} in YAB (the symbols and solid curve indicate experimental data and calculated values based on fitted parameters, respectively).

Table 2. Optical line positions (nm) of Ce in YAB single crystals measured at 300 K (in parentheses the corresponding values for polycrystalline samples are given [5, 6]).

Absorption	—	210	252	272	323
Excitation	—	210	255	273	324
	(−, 200)	(−, 210)	(255, 253)	(273, 272)	(323, 323)
Emission	347	372			
	(344, 338)	(368, 364)			

can be satisfactorily described by a single-exponential decay representing a dominant Orbach process of the spin–lattice relaxation:

$$\Delta H = \Delta H_0 + A\exp^{-\Delta E/kT}\,. \tag{2}$$

The energy difference determined is optimized with $\Delta E = 270 \pm 16$ cm^{-1}, $A = 6500 \pm 1300$ mT and the half-width relating to $T = 0$ is $\Delta H_0 = 1.53 \pm 0.3$ mT. The ground state of Ce is $^2F_{5/2}$, which is split in an axial crystal field into three Kramers doublets. EPR is observed between the levels of the lowest-lying Kramers doublet; however, the observed Orbach lattice relaxation process indicates that the second-lowest Kramers doublet is also involved and the energy difference of these is 270 cm^{-1}. To justify this explanation, we have conducted optical studies of the YAB:Ce single crystal.

3.2. Absorption and photoluminescence in YAB:Ce single crystal

Figure 6 shows the optical absorption of YAB:Ce single crystal at 300 K where four different bands at 210, 252, 272 and 323 nm are observed. The optical absorption band positions agree with those of the four excitation bands at 210, 255, 273 and 324 nm (figure 7) measured at 300 K. Exciting into each absorption band, two emission bands at 347 and 372 nm were detected in the UV range at 300 K (figure 8). The positions of these bands (table 2) are basically the same as for polycrystalline material [5, 6]. The most energetic absorption and excitation band at 200 nm, which was very weak even in [6], could not be observed with our photoluminescence spectrometer which has a limit of 200 nm.

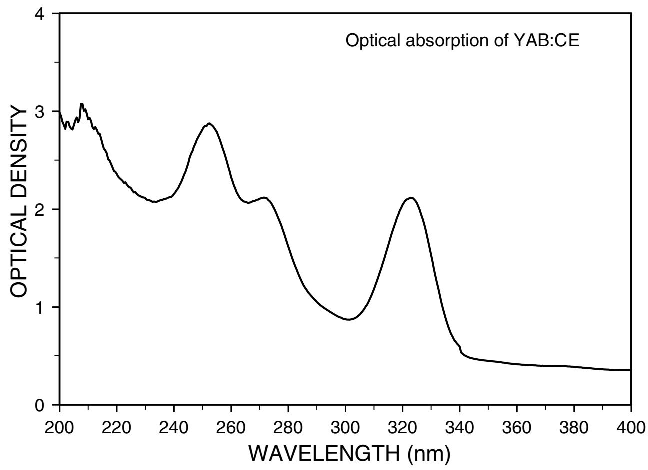

Figure 6. Optical absorption of Ce^{3+} in a YAB single crystal measured at 300 K.

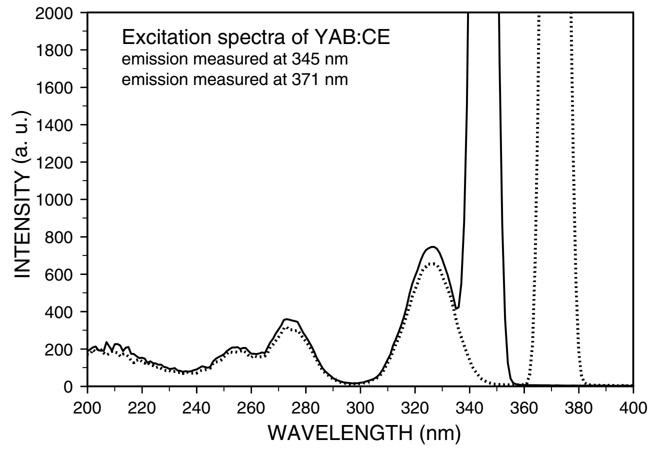

Figure 7. Excitation spectra of Ce^{3+} in a YAB single crystal measured at 300 K. The emission is measured either at 345 nm (solid curve) or at 371 nm (dotted curve).

In order to study further splittings of the emission band to the $^2F_{5/2}$ state, high-resolution polarized emission measurements were made at 4.2 K (figure 9). Three different bands were found: two σ-bands for $\boldsymbol{E} \perp [0001]$ and one π-band for $\boldsymbol{E} \parallel [0001]$.

The schematic energy level system of Ce^{3+} in YAB is shown in figure 10, assuming either D_{3h} or D_3 symmetry. The excited state ^2D is expected to be split into five levels by the crystal field and spin–orbit interactions. The crystal field splits the ground state $^2F_{5/2}$ into three doublets. Since these splittings are small, at 300 K they cannot be resolved. The structure of $^2F_{7/2}$ is not discussed here. The absorption and excitation bands (arrows pointing up in figure 10) correspond to the transitions from the ground level to each of the excited levels of the ^2D state. The emission bands measured at 300 K with low resolution (arrows pointing down in figure 10) correspond to the transitions from the lowest-lying excited state to the $^2F_{5/2}$ and $^2F_{7/2}$ states. However, our polarized photoluminescence measurements with high resolution at 4.2 K indicate that $^2F_{5/2}$ state has three components as expected: the second level is located

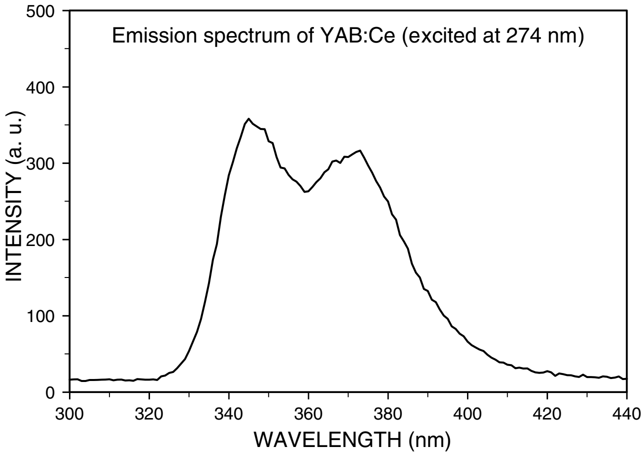

Figure 8. The emission spectrum of Ce^{3+} in a YAB single crystal excited at 274 nm measured at 300 K.

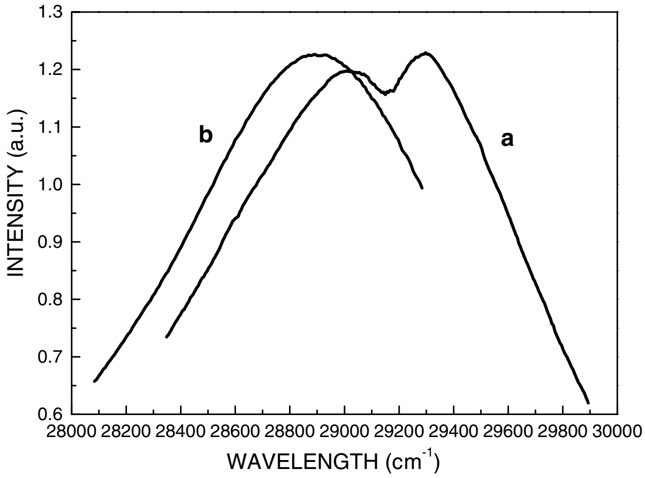

Figure 9. Polarized emission spectra of YAB:Ce single crystal measured at 4.2 K with high resolution (0.15 nm); (a) $\boldsymbol{E} \perp [0001]$ and (b) $\boldsymbol{E} \parallel [0001]$.

$277 \pm 18\ \mathrm{cm}^{-1}$ above the first one and the third level is located $140 \pm 10\ \mathrm{cm}^{-1}$ above the second one. The separation of the two lowest levels is in excellent agreement with that obtained from EPR.

4. Conclusions

For each of the Ce^{3+}, Er^{3+} and Yb^{3+} ions, only one EPR spectrum is measured showing axial symmetry, indicating that all observed dopants replace Y^{3+} ions for the given small dopant concentrations. The **g**-tensors and for Er and Yb also HF interactions are determined (^{167}Er: $I = 7/2$, abundance 22.9%; ^{171}Yb: $I = 1/2$, abundance 14.4%; and ^{173}Yb: $I = 5/2$, abundance 16.2%). From EPR angular variations the corresponding $\tilde{\mathbf{g}}$- and HF $\tilde{\mathbf{A}}$-tensors are determined. The EPR linewidth of Ce broadens and the intensity decreases with increasing temperature due to an Orbach relaxation process. Fitting the curve with an exponential, the energy difference is found to be equal to $270 \pm 16\ \mathrm{cm}^{-1}$.

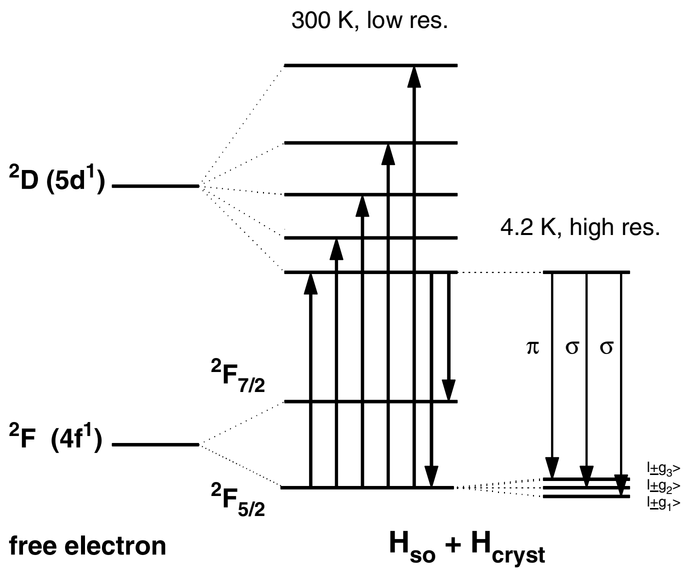

Figure 10. The schematic energy level system for Ce^{3+} for D_{3h} or D_3 symmetry.

The optical absorption and excitation spectra of Ce in YAB single crystal measured at 300 K clearly indicate the presence of four bands and are similar to those found for polycrystalline materials. The emission spectrum consists of two bands measured at 300 K due to transitions from the lowest level of the excited state ^2D to the ground states $^2F_{5/2}$ and $^2F_{7/2}$, respectively. Polarized emission measured at 4.2 K with high resolution, corresponding to the transition from the lowest excited state to the $^2F_{5/2}$ state, relates to splitting of the ground state into three levels. The second level is located 277 ± 18 cm^{-1} above the first one, which is in excellent agreement with the EPR linewidth broadening result. The third level is located 140 ± 10 cm^{-1} above the second one.

Acknowledgments

This research was partly supported by the National Science Research Fund (OTKA, Hungary, Grant Nos T-22859, T-34176 and T-37669) and the Centre of Excellence Programme (Contract No ICAI-2000-70029 EU).

References

[1] Moncorge R, Merkle L D and Zandi B 1999 *Mater. Res. Soc. Bull.* **24** 21
[2] Jaque D, Capmany J, Luo Z D and Garcia Sole J 1997 *J. Phys.: Condens. Matter* **9** 9715
[3] Földvári I, Beregi E, Munoz A, Sosa R and Horváth V 2002 *Opt. Mater.* **19** 241
[4] Wang P, Dawes J M, Dekker P, Knowles D S and Piper J A 1999 *J. Opt. Soc. Am.* B **16** 63
[5] Blasse G and Bril A 1967 *J. Chem. Phys.* **47** 5139
[6] Aloui-Lebbou O, Goutaudier C, Kubota S, Dujardin C, Cohen-Adad M Th, Pédrini C, Florian P and Massiot D *Opt. Mater.* **16** 77
[7] Knitel M J, Dorenbos P, van Eijk C W E, Plasteig B, Viana B, Kahn-Harari A and Vivien D 2000 *Nucl. Instrum. Methods* A **443** 364
[8] Belokoneva E L, Asisiv A V, Leonuk N I, Simonov M A and Belov N B 1981 *Zh. Strukt. Khim.* **22** 196
[9] Blasse G, Bril A and Nieuwpoort W C 1966 *J. Phys. Chem. Solids* **27** 1587